Quantum grid infrared photodetectors

L. P. Rokhinson,[a)] C. J. Chen, and D. C. Tsui
Department of Electrical Engineering, Princeton University, Princeton, New Jersey 08544

G. A. Vawter
Sandia National Laboratories, Albuquerque, New Mexico 87185-0603

K. K. Choi
U. S. Army Research Laboratory, 2800 Power Mill Road, Adelphi, Maryland 20783

(Received 11 September 1998; accepted for publication 1 December 1998)

In this letter we introduce a quantum well infrared photodetector (QWIP) structure, which we refer to as the quantum grid infrared photodetector (QGIP). In an ideal structure, a grid pattern with very narrow linewidth is created in the QWIP active region to achieve lateral electron confinement, thereby improving its absorption as well as transport characteristics. In order to realize this detector structure, we have fabricated QGIPs with line patterns of lithographical linewidths w_l ranging from 0.1 to 4 μm, allowing for possible sidewall depletion. Low-damage reactive ion beam etching was employed to produce vertical sidewalls. From the experimental data, although the best detector performance occurs at $w_l \approx 1.5$ μm, the detector starts to improve when $w_l < 0.5$ μm, indicating a possible quantum confinement effect. © *1999 American Institute of Physics.*
[S0003-6951(99)04005-X]

Quantum well infrared photodetectors (QWIPs) using GaAs/AlGaAs multiple quantum wells (MQWs) have matured rapidly in the last several years.[1] Most of the detector parameters have been optimized. However, issues related to the coupling of normal incident radiation are still not satisfactory and need to be improved. It is well known that dipole selection rules forbid absorption of photons polarized in the plane of the wells. In order to realize focal plane detector arrays, different light coupling schemes were tried. Gratings[2–4] provide efficient light coupling for large area devices but suffer from spectrum narrowing effects and decreased coupling efficiency for small devices. A corrugated QWIP (C-QWIP) coupling scheme[5] relies on light reflection rather than diffraction and does not have strong wavelength and detector size dependence. C-QWIP was shown to have high quantum efficiency; multicolor detectors[6] and focal plane arrays[7] were successfully demonstrated. However, C-QWIP has certain limitations; for example, it can only couple to one polarization of light.

In order to solve the problem of polarization fundamentally, attempts have been made to produce lateral electron confinement, in addition to the usual vertical confinement by the material layers. One such approach is to create quantum dot structures using three-dimensional material growth techniques.[8] In this work we used electron beam lithography and low-damage reactive ion beam etching (RIBE)[9] to produce submicron size features on a conventional optimized QWIP to achieve possible normal incident absorption. The detector structure is referred to as the quantum grid infrared photodetector (QGIP). This approach may produce a more uniform and optimized detector array than the other approaches. In a QGIP, either a linear, dotted, or crossed grid pattern is etched into the detector active region (see Fig. 1). Therefore, in addition to the possible intrinsic normal incident absorption due to lateral confinement, the structure also utilizes the diffraction effect of the grid, similar to that proposed by Schimert *et al.*[10] Furthermore, lateral confinement will also potentially increase the photoelectron lifetime and, hence, the photoconductive gain of the detector by reducing the available electron states for phonon scattering.

The QWIPs used in this work were grown by molecular beam epitaxy (MBE) on a semi-insulating (001) GaAs substrate. The active region, which is sandwiched between 5000 Å n-GaAs for the top and 10 000 Å for the bottom contacts, consists of 20 periods of 500 Å $Al_{0.30}Ga_{0.70}As$ barriers and 50 Å n-GaAs wells. The doping density of the contacts is 1.0×10^{18} cm^{-3}. In our approach there is an uncertainty to the extent of the depletion at the exposed sidewalls of the grid due to the air–GaAs surface bandbending. In order to obtain different depletion width w_d, QGIPs have been fab-

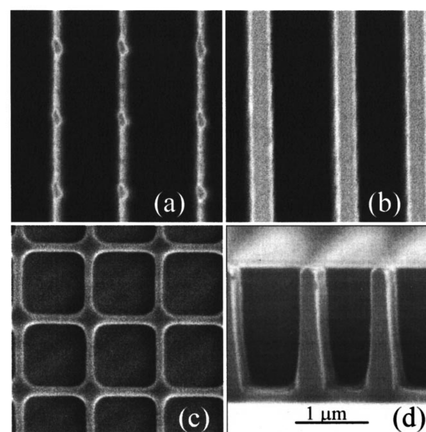

FIG. 1. SEM micrographs of QGIP devices with (a) dotted, (b) linear and (c) crossed grid patterns. In (d) cross section of the linear grid QGIP is shown. All images are 3 μm×3 μm.

a)Electronic mail: leonid@ee.princeton.edu

 © 1999 American Institute of Physics

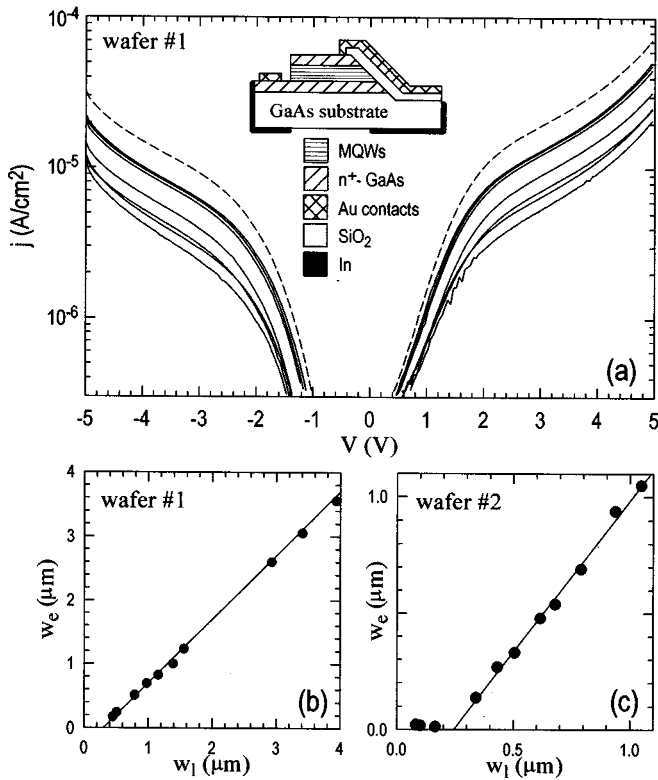

FIG. 2. (a) Dark current characteristics of the samples from wafer No. 1 with $w_l = 0.51$, 0.80, 1.0, 1.16, 1.39, 1.56, 3.0, 3.5 and 4.0 μm measured at 77 K (solid curves from bottom up). The dashed curve is dark current in the 45° reference sample. The sample cross section is shown in the inset. In (b) and (c) electrical linewidth w_e is plotted as a function of the lithographical width w_l for the samples from wafer Nos. 1 and 2. Solid lines are linear fits to the data for $w_l > 0.2$ μm. The difference between w_l and w_e is twice the depletion width $2w_d$.

ricated from a wafer with a usual optimized doping density of 0.5×10^{18} cm^{-3} in the wells (wafer No. 1) as well as from a wafer with ten times higher doping density (wafer No. 2).

Sample processing can be divided into four steps. First, top and bottom contacts were defined by optical lithography. In order to reliably compare samples with different pattern sizes, we minimized the current contribution from the top contact pad by etching the active region below the pad down to the insulating substrate. The contact was achieved by forming a narrow metal bridge which goes over the edge of the etched region and forms an Ohmic contact to the top layer, see the inset in Fig. 2(a). The electrical junction was protected from shorting by 1300 Å of deposited SiO_2. The bridge area, which contributes to both dark and photocurrent, is 10×15 μm^2 and is negligible compared to the 146×146 μm^2 pattern size. For the bottom contact a square was etched down to the bottom *n*-GaAs layer. Au/Ge contacts were alloyed at 360 °C for 15 s and protected with 1800 Å of Ni for the further processing.

In the second step, electron beam lithography and subsequent lift-off of 1200 Å of Ni were used to define lines of different width and spacing. Lithographical linewidth w_l was varied from 0.1 up to 4 μm in different samples. Line spacing alternated from $s-0.1$ μm and $s+0.1$ μm in each sample; $s=1.0$ μm for the samples from wafer No. 1 and 0.7 μm$<s<1.0$ μm for the samples from wafer No. 2. Control samples with no line pattern (filled 146×146 μm^2 square) were also prepared.

Low-damage RIBE etching with Ni acting as an etch mask is described elsewhere.[9] The etching produces almost vertical walls [Fig. 1(d)] and very high depth-to-width aspect ratios of up to 17 were achieved. The Ni mask also acts as a reflector and increases the number of light passes within the lines by a factor of 2. As the last step, each detector was cut into a separate device and all edges were covered with indium in order to eliminate possible cross-talk between devices and photoresponse from the light reflected at the edge into the device area at some angle. Thus, we insure that the measured photoresponse is a measure of the coupling efficiency of the normal incidence light. A sample with a filled square pattern and an edge facet polished at 45° (45° reference) was prepared as a reference. Although the pattern can be linear, crossed grid or lines with dots (Fig. 1), the data presented below are exclusively from the linear patterns.

Dark current characteristics for several samples, measured at 77 K, are shown in Fig. 2(a). The current density scales with the active device area uniformly, independent of the applied voltage. From this scaling we can determine an electrical width of the lines, $w_e = j/j(45°)L/N$, where j is the dark current, $j(45°)$ is the dark current in the 45° reference, N is the number of lines, and $L=146$ μm is the nominal width of our devices. Lithographical width, w_l, of the lines was determined from scanning electron microscope (SEM) micrographs of the actual devices. Electrical width versus lithographical width is plotted in Figs. 2(b) and 2(c). The difference between w_l and w_e is twice the depletion width $2w_d = w_l - w_e$. In wafer No. 1, $w_d \approx 1500$ Å, independent of the linewidth (a linear fit has a slope 1.0). In wafer No. 2, w_d is smaller than that in wafer No. 1 due to a much higher doping density. By extrapolating the fits in Figs. 2(b) and 2(c) to $w_e=0$, we estimate an electrical pinch-off to occur for $w_l<3000$ Å in wafer No. 1 and for $w_l<2200$ Å in wafer No. 2. However, for the samples with $w_l<2200$ Å from wafer No. 2, current and, thus, w_e, are nonzero.

Photocurrent was measured at 10 K using a prism spectrometer and a calibrated 1200 °C source. Spectra from different samples were normalized to the maximum value and compared to the spectrum of the 45° reference. For samples with w_l ranging from 0.1 to 4.0 μm, the spectra were found to be identical to the one measured in the 45° reference; no line narrowing effects were observed. Thus, the measured spectra reflects the intrinsic characteristics of the MQWs and this result shows that the introduced coupling scheme can be used for broadband and multicolor detection.

For characterization of the coupling efficiency, responsivity ratio, R, defined as the ratio of the peak responsivity of the sample to the peak responsivity of the 45° reference, is often chosen as a figure of merit. Since our samples do have different amounts of material removed we normalized R by the corresponding dark current ratio $f=j/j(45°)$. R/f for different w_l are plotted in Fig. 3. $R/f=1$ means that the coupling efficiency is as good as that of the 45° reference with two light passes. The worst coupling efficiency (17%) was measured for the sample with no special coupling (i.e., a filled square placed perpendicular to the light direction). From Fig. 3, the maximum R/f is obtained when $w_l \approx 1.5$ μm, at which $R/f=130\%$ of the 45° reference. This maximum is expected from the grating equation $\lambda = np$ for

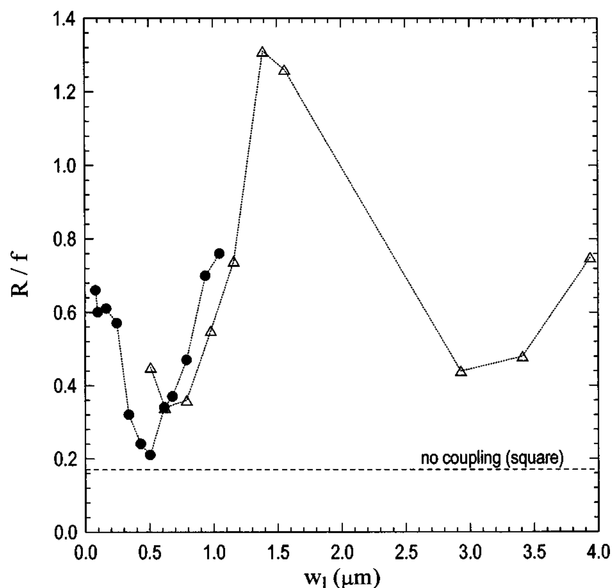

FIG. 3. Coupling efficiency (R/f) is plotted as a function of the linewidth w_l. △ and ● are for the samples from wafer Nos. 1 and 2, respectively. Dashed line is the ratio for the sample with no special coupling (filled square placed perpendicular to the light direction).

the first-order diffraction at 90° with a grating period $p = w_l + s = 2.5\ \mu m$, $\lambda = 7.6\ \mu m$ and the refractive index $n = 3.1$. At this periodicity, the grid serves as an efficient diffraction grating for the incident light at the peak wavelength. Similarly, a second maximum is at $w_l = 4.0\ \mu m$ ($p = 5.0\ \mu m$) for the second-order diffraction.

For a diffraction grating we expect the detector responsivity to decrease rapidly for $w_l < 1.5\ \mu m$ ($p < 2.5\ \mu m$) due to low diffraction efficiency. Indeed, R/f decreases down to 0.2 at $w_l = 0.5\ \mu m$. However, for $w_l < 0.6\ \mu m$ in wafer No. 1 and $w_l < 0.5\ \mu m$ in wafer No. 2, R/f starts to increase as w_l is further reduced. This increase is not predicted from diffraction effects. We attribute it to an enhancement in detectivity from lateral confinement of the electrons in the quantum wires. In order to confirm that smaller linewidth, not a change of the period, is responsible for the R/f enhancement, we prepared several samples with the same period but different linewidths: samples with $w_l = 0.082$ and $0.1\ \mu m$ have $p = 1.0\ \mu m$ and samples with $w_l = 0.165$ and $0.248\ \mu m$ have $p = 1.1\ \mu m$. It is clear from Fig. 3 that the samples with narrower w_l do indeed have R/f higher than the samples with the same p but larger w_l.

In summary, we have proposed an approach, the QGIP, to achieve lateral confinement for electrons in QWIPs. With submicron lithographic techniques, two-dimensional or three-dimensional quantum confined structures can be obtained, with better uniformity, reproducibility and size control. We have systematically characterized QGIPs with different periodicity and doping densities. From this study, we determined the optimized grid parameters for efficient diffraction, and compared this coupling scheme to the 45° coupling standard. We have also determined the depletion width along the sidewalls of the grid. We observed increasing detector performance with decreasing linewidth for $w_l < 0.5\ \mu m$ that can be attributed to lateral quantum confinement effects. Work is under way to further reduce the linewidth to enhance quantum confinement.

The work at Princeton University is supported by the ARO. Sandia National Laboratories is a multiprogram Laboratory operated by Sandia Corporation, a Lockhead-Martin Company, for the United States Department of Energy.

[1] K. K. Choi, *The Physics of Quantum Well Infrared Photodetectors* (World Scientific, River Edge, NJ, 1997).
[2] G. Hasnain, B. F. Levine, C. G. Bethea, R. A. Logan, J. Walker, and R. J. Malik, Appl. Phys. Lett. **54**, 2515 (1989).
[3] J. Y. Anderson, L. Lundqvist, and Z. F. Paska, Appl. Phys. Lett. **58**, 2264 (1991).
[4] J. Y. Anderson and L. Lundqvist, Appl. Phys. Lett. **59**, 857 (1991).
[5] C. J. Chen, K. K. Choi, M. Z. Tidrow, and D. C. Tsui, Appl. Phys. Lett. **68**, 1446 (1996).
[6] C. J. Chen, K. K. Choi, W. H. Chang, and D. C. Tsui, Appl. Phys. Lett. **72**, 7 (1998).
[7] K. K. Choi, A. C. Goldberg, N. C. Das, M. D. Jhabvala, R. B. Bailey, and K. Vural, Proc. SPIE **3287**, 118 (1998).
[8] D. Pan, E. Towe, and S. Kennerly, Electron. Lett. **34**, 1019 (1998).
[9] J. R. Wendt, G. A. Vawter, R. E. Smith, and M. E. Warren, J. Vac. Sci. Technol. B **13**, 2705 (1995).
[10] T. R. Schimert, S. L. Barnes, A. J. Brouns, F. C. Case, P. Mitra, and L. T. Claiborne, Appl. Phys. Lett. **96**, 2846 (1996).